2022

A comparison of predicted and observed ocean tidal loading displacements around the Puget Sound

Tanessa Caitlyn Morris
University of Montana, Missoula, tanessa.morris@umontana.edu

A comparison of predicted and observed ocean tidal loading displacements around the Puget Sound

By Tanessa Morris

Advisor: Dr. Hilary Martens

This material is based upon work supported by the National Aeronautics and Space Administration under Grant Number 80NSSC21K0837.

Table of Contents

A comparison of predicted and observed ocean tidal loading displacements around the Puget Sound

Abstract

Around coastlines and in shallow oceans, models of ocean tidal loading (OTL) are not highly accurate and can create sources of error in OTL analysis. OTL is tides moving ocean water that cause the surface of Earth to deform. In this study, forward-modelled predictions of OTL are compared to observations from Global Navigation Satellite System (GNSS) data to explore the elastic deformation response of Earth to OTL around the Puget Sound. Data from 75 stations were processed to yield position estimates at intervals of 5 minutes for a year. The OTL model used for comparison was the FES2014b ocean-tide model loading a spherically symmetric, non-rotating, elastic, and isotropic (SNREI) Earth model. The three tidal frequency bands used were the semidiurnal (M_2), diurnal (O_1), and fortnightly (M_f). The M_2 tide is the largest and M_f the smallest. The model and observations have the largest residual displacements of 5 mm for the M_2 tide, and the smallest 2 mm for the O_1 tide. The particle motion residuals have strong spatial coherence in the M_2 and O_1 tide but are less coherent with the M_f tide. These residuals indicate that either the models of OTL and/or the observations of OTL have deficiencies. Model deficiencies are likely due, in part, to the FES2014b model not extending fully into and accounting for the complex morphology of the Puget Sound. Another element explored was quantifying the difference in observed OTL when a sidereal filter is applied to the GNSS time series. A sidereal filter is used to remove multipath errors that occur every sidereal day when GNSS satellite orbits repeat. The largest residual displacements were 1 mm in the M_f tidal band and the smallest 0.5 mm in the M_2 band. These differences can alter the observations used in

OTL analysis, which impacts model comparisons. Multipath errors can overlap in frequency space with tidal frequencies, so the use of a sidereal filter must be carefully considered before its application.

Introduction

The Earth crust is commonly viewed as being a rigid entity; however, the crust is elastic and deforms due to loading on it. Tides moving ocean water cause the surface of Earth to deform. This is known as ocean tidal loading (OTL). The water is a surface load that modifies the shape of Earth's surface due to its weight (Martens et al., 2016b; Jentzsch, 2005). The deformation is controlled by the properties of the Earth's crust and mantle (Martens et al., 2016a). Ocean tide heights can range from the order of millimeters to meters and surface displacement can generally be as large as centimeters. The largest ocean tide displacements are seen along the coasts (Ito & Simons, 2011).

A method to measure surface displacement is the use of Global Navigation Satellite Systems (GNSS) (Agnew, 2015; Martens & Simons, 2020). GNSS are constellations of satellites that provide position and timing of antennas. This is accomplished by satellites sending a signal to a GNSS receiver; the receiver will receive the signal and the time interval that it takes for this to happen can be used to determine a position (Lichtenegger et al., 2008). GNSS includes the Global Positioning System (GPS), which refers only to the North American delegation of satellites. GNSS data includes GPS, but also GLONASS, Galileo, and other international satellite systems (Lichtenegger et al., 2008). A GNSS station consists of a receiver, an antenna, and receives data from several satellites. Ideally, timing data is received from at least 4 or 5 satellites at a time. GNSS is commonly used to analyze tectonic changes. GNSS data can also be

processed and analyzed to investigate Earth's structure and dynamics. The GNSS data can be used, for example, to estimate crustal strain, which is often related to tectonics, but can be associated with other processes as well (Jentzsch, 2005; Lichtenegger et al., 2008; Atkins & Ziebart, 2015). The GNSS stations can move as a result of surface strain and movement, and these changes are recorded by the GNSS station itself. The locations of the GNSS stations used in this project are shown below in Figure 1. GNSS provides high resolution continuous sampling, has a high global density of receivers, and allows the capability to use processing methods that produce precise surface displacement series (Agnew, 2015; Martens et al., 2016a; Martens et al., 2016b). GNSS data can be discrete measurements taken at a moment in time (campaign style) or can be collected as continuous data over a sampling period. This study utilizes Network of the Americas (NOTA) GNSS stations (e.g., Herring et al. 2016).

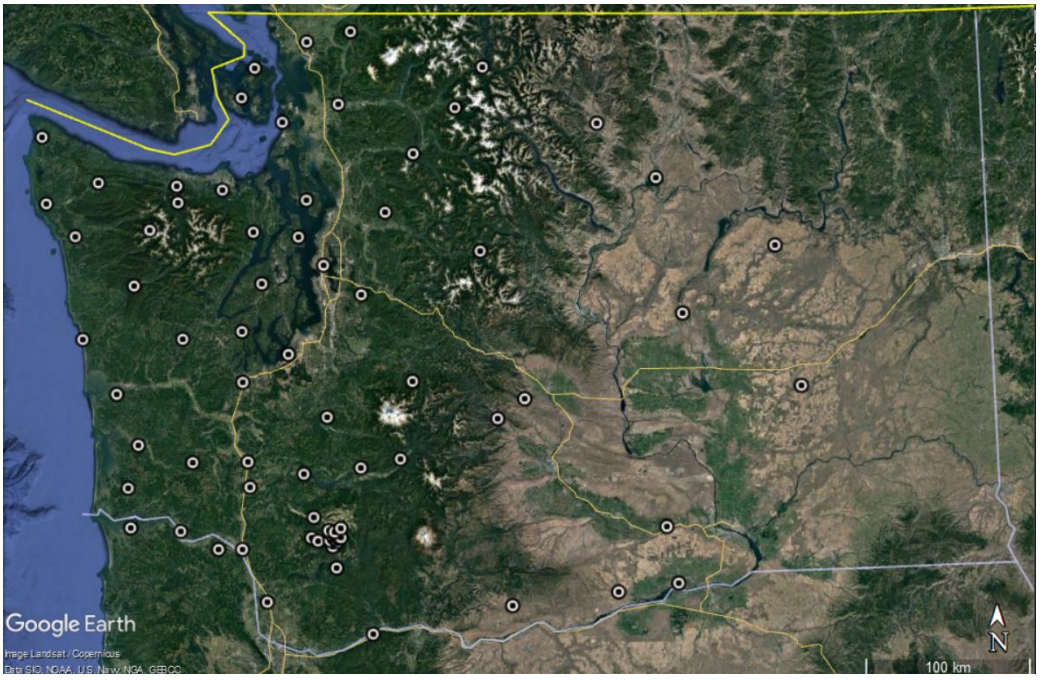

Figure 1: Map showing all stations used in this study. All stations are marked by the black and white points. Credit: Google Earth Pro.

There are two main types of tides: body tides and ocean tides. Body tides are also called solid Earth tides, Earth tides, or crustal tides. These tides are caused directly by the gravity of the sun and moon acting on the solid Earth (Wahr, 1981; Brosche et al., 1978). Body tides are highly predictable with typical periods longer than 12 hours and amplitudes of about a meter (Wahr, 1981; Zschau, 1978). Body tides are also influenced strongly by deep-Earth properties. The internal structure of Earth also influences body tides and how the crust is able to move and deform (Pugh & Woodworth, 2014; Martens & Simons, 2020; Ito & Simons, 2011). Ocean tides are not as predictable as body tides, as they are influenced by the shape of coastlines, the shape of the ocean floor, and the depth of the ocean (Pugh & Woodworth, 2014; Jentzsch, 2005). Barriers such as the continent-ocean interaction and ocean bathymetry change tidal flows and constrain how the water is allowed to move. These tides are present at many different wavelengths. This spatial variation of ocean tides and their impacts allows Earth's structure to be analyzed at different spatial wavelengths (Martens & Simons, 2020). Analyzing Earth structure at varied spatial wavelengths can provide insight into processes such as mantle convection and plate tectonics.

Ocean tide models can be refined through the modelling of the surface displacements of the Earth's surface. Observations of OTL can be used to refine models of Earth's structure and ocean tides. There are areas where the observed OTL is different from the predictive models of the same area. The ocean tide models in the deep ocean are highly accurate, due to accurate satellite measurements (Martens et al., 2016b; Bos et al., 2015). Around coastlines and in the shallow ocean, the ocean tide models are not as accurate and are a source of error in OTL analysis (Ito & Simons, 2011). These models are not as accurate because satellite measurements are difficult in these areas and there are non-linear effects that need to be considered (Pugh &

Woodworth, 2014). Another cause of the error with the models is that the resolutions used are not small enough for intricate coastlines (Pain et al., 2005). The models are typically on regular grids, which do not allow for accurate geometries and resolution for coastline analysis. The Puget Sound is an example of an area where OTL models can be improved. In this study, predictions of OTL based on the FES2014b ocean tide model are going to be compared to observed OTL in the Puget Sound and the differences will be computed.

Another element that is explored in this study is the impact the application of a sidereal filter has on the observations of OTL. A sidereal filter is used to remove multipath errors (Choi et al., 2014). A multipath error occurs when two radio waves have travelled different path lengths between the receiver and the transmitter (Zhdanov, 2002). The signals caused by multipath effects may overlap in frequency space with the tidal signals. This overlapping could amplify or diminish tidal signals. The difference in paths taken is shown in Figure 2. This can occur due to errors in signal reception, but it also occurs when emitted waves are interfered with. This interference can occur when waves are diffracted or reflected by elements in the environment (Zhdanov, 2002; Atkins & Ziebart, 2014). The radio waves travel longer than they would have if it were a direct line from transmitter to receiver. For example, if there is a tall tree next to the satellite receiver, the radio waves can deflect off this tree before reaching the receiver. This reflection alters the length of path taken by the radio waves, creating a multipath error, as the waves have travelled longer than normal (Dong et al., 2015; Hannah, 2001). Multipath errors can alter GPS positions produced. The geometry of satellites repeats approximately every sidereal day (Choi et al., 2014). A sidereal day is the amount of time for the earth to rotate 360 degrees, which is usually 23 hours, 56 minutes, and 4 seconds (Zhdanov, 2002). A sidereal filter removes multipath errors that occur daily (Choi et al., 2014; Atkins & Ziebart, 2015). It

minimizes the error in positioning (Atkins & Ziebart, 2014). While this can prove an effective tool in improving the accuracy of GPS positioning, it can also be argued that multipath errors can manipulate an OTL analysis due to overlap in frequency space.

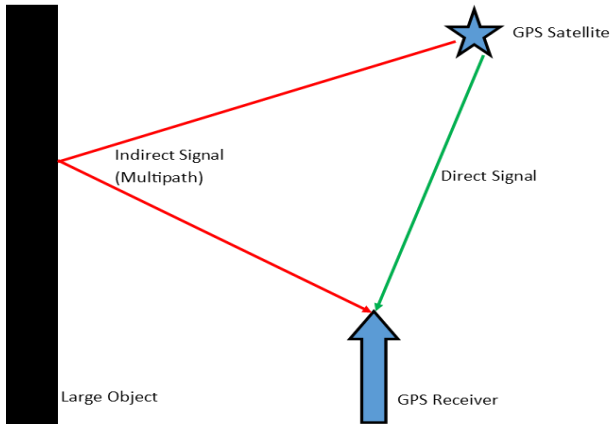

Figure 2: Multipath errors compared to a direct signal from a satellite. The multipath signal must travel much further than that of the direct signal, altering the recorded position of the receiver.

This work is focused on the Puget Sound area and the impact that ocean tidal loading across three frequency bands has on this area. The Puget Sound is an inlet of the Pacific Ocean located in Washington and is shown in Figure 3. The data has been collected continuously at sub minute intervals over the course of a year. The raw GNSS data was processed to provide a time-series of surface displacements at 5-minute intervals. These displacements are provided in the directions up, north, and east. The amplitude and phase of tidal harmonics were determined using tidal harmonic analysis (Martens et al., 2016; Martens & Simons 2020). The OTL observations are compared to predictive models in three frequency bands. The three bands used are semidiurnal (M_2), diurnal (O_1), and fortnightly (M_f). The M_2 tide peak occurs twice per day, O_1 once per day, and M_f once every two weeks (Agnew, 2015; Martens et al., 2016a; Martens et

al., 2016b). The M_2 tide changes spatially at the greatest rate (Brown, Hutchinson, 1989). The most prominent of these tides is M_2 and the least is M_f. The observed OTL is compared to the predictive models of OTL, with the goal to refine the tide models. Predictions are made using the LoadDef software (Martens et al., 2019). LoadDef is a Python toolkit that is used to model elastic deformation by surface loading on spherically symmetric bodies. I hypothesize that the M_2 tide will show the greatest residuals between the observed OTL and predicted OTL, due to its larger amplitude. There is also a comparison of a sidereal filter applied versus not being applied. The difference between a sidereal filter and lack thereof is quantified.

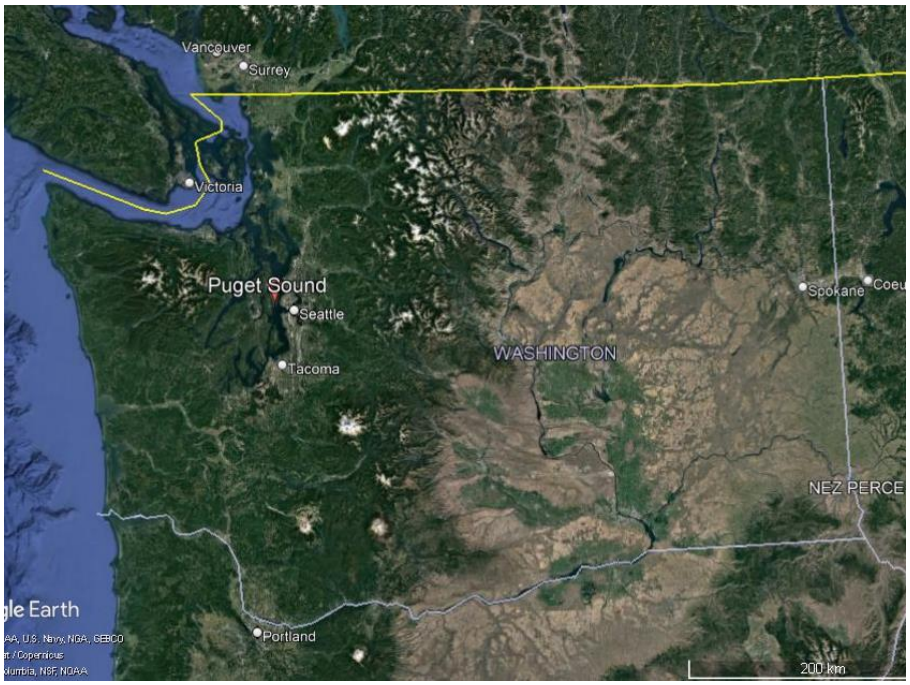

Figure 3: The Puget Sound area as well as the Pacific Ocean and major cities in Washington to provide a context as to where this research is being performed. The Puget Sound has a complex coastline. Credit: Google Earth Pro.

The ocean tidal loading in the western United States has previously been explored by Ito & Simons (2011), albeit not targeted at the Puget Sound. There has been research done on a high-resolution tidal model for the Northeast Pacific Ocean; however, this research included the effects of all tidal constituents, including body tides and tidal potential (Foreman et al., 2000). This work also focused more on Alaska than the area of the Puget Sound. The tidal energy has been explored to create a tidal energy project by Polagye and Thomson in 2013. However, this research was focused on the energy of the tides, not how the tides impacted Earth surface deformation. Similar studies as this have been performed in Alaska (Martens & Simons, 2020), South America (Martens et al., 2016a), and Europe (Bos et al., 2015; Penna et al., 2015). In each case, the (an)elastic response due to OTL was studied and compared with predicted OTL deformation. To our knowledge, this is the first dedicated and detailed study of OTL in the Puget Sound.

Motivation

The motivation behind this work is to quantify the differences in surface displacements between the models of surface displacement due to OTL and observations of OTL. I am interested in complex coastlines and unique geographic regions, such as the Puget Sound. The Puget Sound has a complex coastline and any existing models of how ocean tides impact this area have not been at a high enough resolution to accurately capture the tidal effects in the Puget Sound. Many of the existing global tidal models do not reach into the Puget Sound. When the model does not cover the Puget Sound and extend into these waters, the OTL models around the Puget Sound are likely not accurate. With a higher resolution of the ocean tides in this area, better decisions can be made regarding both the ecosystem dynamics and human projects. These can include projects

such as building tall structures or the introduction of a new plant or animal species to the area that can be influenced by the tides. Observations of OTL could be used to refine tide models in the Puget Sound. Those that rely on the ocean for their livelihoods, such as those in the oilfield industry, shipping, and fishing, can potentially benefit from better models of the local ocean tides. We therefore seek to determine deficiencies in the tide models so that they can later be improved by GPS data. This study will quantify the difference between observed OTL and modelled OTL to determine where deficiencies exist, such as lack of coverage deficiencies or poor resolution deficiencies in the Puget Sound, so that these can potentially be improved in future models with constraints from GNSS observations of OTL.

Another motivation in this project is to determine how much of an impact a sidereal filter has in GNSS data processing and to quantify the difference in observed OTL when applying a sidereal filter or not. If small differences are observed, it would seem it is not worth applying a sidereal filter, and it would not necessarily need to be considered. Small differences are differences that fall below the current measurement-precision capabilities of GNSS, or that do not alter the observations of OTL enough to significantly reduce the differences between the predictions and the observations relative to the magnitude of the load tides. However, with significant differences (e.g., >5-10%), more research and consideration may need to be made to determine whether it is appropriate to use for future projects. It is important to quantify the effect a sidereal filter has on observations of OTL displacement because if the observations are modified by applying the filter (or by not applying the filter), then the comparison between the observations and predictive models will be changed as well. The sidereal filter overlaps in frequency space with the main tidal frequencies, so special care must be taken regarding the filter. If observations are altered, then residuals between model and observations are also altered.

Methods

Data Selection

Initially all GPS stations in the western United States were considered and analyzed to determine the impacts OTL has on the Western United States. After some analysis and research, it was decided that this work would focus on the Puget Sound area, as there are no detailed OTL studies done on this complex area (to our knowledge). To capture the full scope of the Puget Sound area, all GPS stations in Washington State were considered and all others were removed. A total of 75 GPS stations were considered. These stations are shown on the map in Figure 1. There is a high concentration of 19 stations located near Mount St. Helens to capture seismic activity, while there are few stations in the eastern part of Washington. The seismic activity is not considered and removed from analysis of the data, but this concentration of stations provides more data points here than in other areas.

The time series data of the stations was then considered to determine which stations should be used in the analysis of the Puget Sound. Figures 4 a and b show examples of stations that were used in the analysis. There is clear harmonic behaviour in the time-series data, and the residuals between the data and a tidal-harmonic fit exhibit a smooth bell curve. The data also appears continuous over the sampling period. These are considered stations with good data that should be used in analysis. Stations were analyzed and if any had poor quality data they were removed from the analysis. Figure 4 c shows an example of data that was poorer in quality. The data are choppier, and the bell curve of residuals has a large peak and is uneven on either side of the peak.

a)

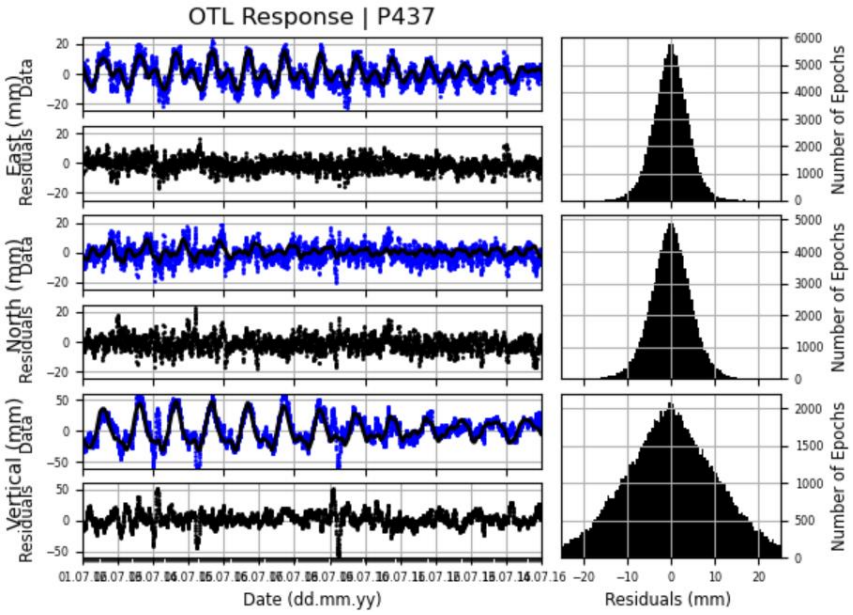
OTL Response | P437
East (mm)
North (mm)
Vertical (mm)
Data
Residuals
Number of Epochs
Date (dd.mm.yy)
Residuals (mm)

b)

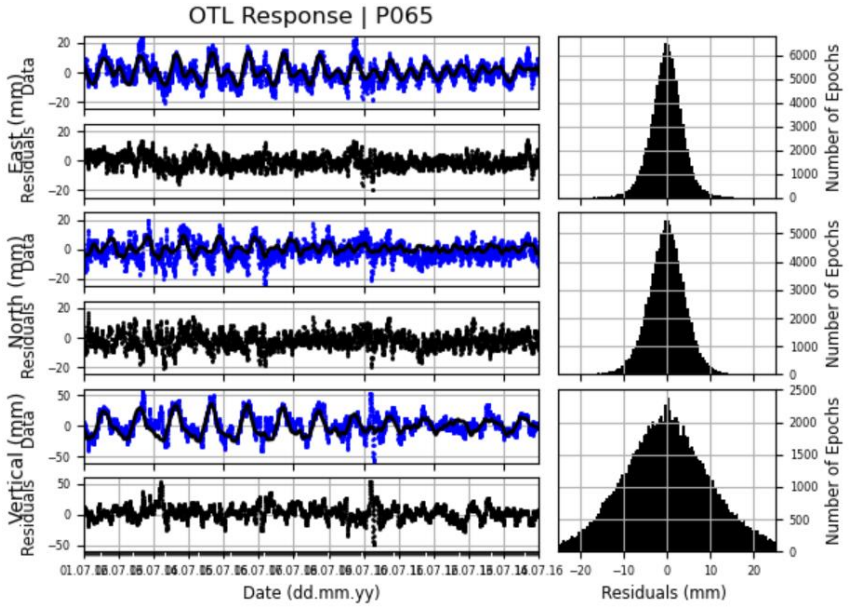
OTL Response | P065
East (mm)
North (mm)
Vertical (mm)
Data
Residuals
Number of Epochs
Date (dd.mm.yy)
Residuals (mm)

c)

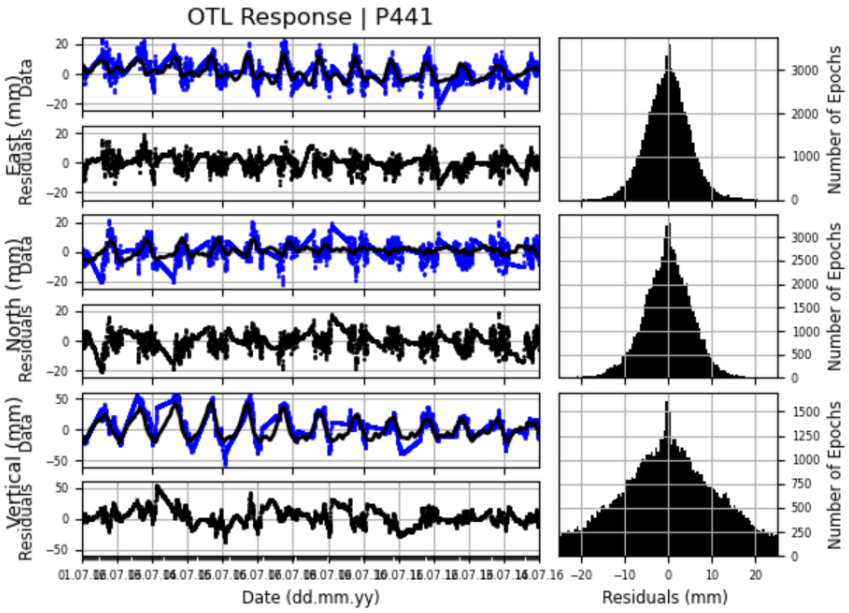

Figure 4: a) time series plots for Station P437, which is located nearest the Puget Sound. This station has good data, as is evident by the clear tidal sine waves and clean distribution. b) Time series plots for Station 065, which also has good data, but this station is located further from the Puget Sound. This station is approximately 160 km from the Puget Sound. c) Time series plots for Station 441, which is a station with poorer quality data and a significant amount of missing data. The normal distribution has sharp peaks, indicating poorer quality data.

Data Filtering

The initial data filtering occurs before the data is analyzed. In the processing of the raw data (using GipsyX; Bertiger et al. 2020) all body tides and pole tides are removed from the data. The ocean load tides are kept for analysis. The position of GNSS stations were estimated using a random-walk procedure. The random-walk procedure is stochastic and is formed by "the successive summation of independent, identically distributed random variables" (Lawler & Limic, 2010). The raw data was processed at time intervals of 5 minutes. Using position

estimates from GipsyX and the offset catalog from UNAVCO (Herring et al. 2016), displacements from significant seismic events are removed. The GipsyX processing and post-processing corrections were performed by Dr. Hilary Martens.

There are also other levels of filtering that can be performed prior to creating and analyzing particle motion ellipses (PME). A PME is the path taken by a GNSS station due to displacement of the earth at a given frequency. The movement of stations are in an elliptical shape and are due to individual harmonics of OTL. These ellipses can be seen in Figure 6. A main filtering technique done in station analysis is in the median absolute deviation (MAD). The MAD designates the number of standard deviations from the running median to consider an outlier for removal (Leys et al., 2013). The three MAD thresholds that were considered in this analysis were 15, 10, and 5. It was determined through running several iterations of these levels that MAD-10 was the most appropriate level at which to compare the predictive model to the observations. At this level, the largest extraneous values are identified and removed from the data, while retaining the valuable data. With a MAD-15 filter too many extraneous values are included, and a MAD-5 filter clips the valuable data. The number of days in an outlier detection window was also considered (WIN). Windows of 7 days, 14 days, and 21 days were considered. It was determined that WIN-14 was the most appropriate, based on the maximum tidal period being a fortnight. WIN-21 was mainly considered because the tide with the longest period is the M_f tide, with a 14-day period. The larger window was considered to ensure that all possible data from the M_f was detected. However, there were no noticeable changes when using WIN-7 or WIN-21, so it was decided to use the 14-day window, WIN-14.

OTL Response Forward Modelling

Forward modelling was performed to compare a model for OTL to the observed OTL. The forward modelling predicts surface displacement in 3 dimensions. The 3 dimensions are up, east, and north, and they are caused by OTL. LoadDef software is used to produce the forward models of the surface displacement. The LoadDef software calculates surface displacement using an ocean-tide model and the radial profile of Earth's structure (Martens et al., 2019). The earth model used was the Preliminary Reference Earth Model (PREM). PREM was developed using a large dataset of normal modes, seismic travel-time observations, and moment of inertia to create a model of the earth (Dziewonski & Anderson, 1981). PREM represents a spherically symmetric Earth. We assume isotropic and elastic properties.

The ocean tide model used was FES2014b. The FES2014b model is highly accurate in deep waters, and the performance of the model was estimated by tidal gauge and altimeter measurements (Carrère et al., 2015). Other models could also be used, but this was the model selected for this analysis. The model was subject to convolution with displacement load Green Functions (LGFs). The first step in using the LoadDef software was to compute the Load Love Numbers (LLN) and the Green's Functions. The results of these computations can be seen in Appendix 1. LLNs are used to characterize the rigidity of the planet and how easily it changes shape due to loading. To calculate the LLNs, the motion equations for spheroidal deformation through Earth's layers were integrated (Martens et al., 2016). LGFs are computed for the vertical and horizontal displacement. This is done by combining the LLNs in spherical-harmonic expansions (Martens et al., 2016; Martens & Simons, 2020). With the LGF values computed, the FES2014b model was convolved with the LGFs to estimate OTL displacement at each station.

The LGFs are convolved with ocean tide models to model the displacement due to the OTL. The convolutions were performed for the M_2, O_1, and M_f tides. We assumed that the ocean-water density is constant at 1030 kg/m^3. This value of sea water density can impact the predictions of OTL displacements, and a value between 1025 and 1035 kg/m^3 is typical. An example of convolution results can be seen below in Figure 5.

Extension/Epoch	Lat(+N,deg)	Lon(+E,deg)	E-Amp(mm)	E-Pha(deg)	N-Amp(mm)	N-Pha(deg)	V-Amp(mm)	V-Pha(deg)		
FES2014-M2	48.01605700	237.07245900	6.19630200	88.77694822	1.82579239	286.97885102	13.30323685	74.77085363		
FES2014-Mf	48.01605700	237.07245900	0.20641726	97.30380654	0.46972202	166.86608177	0.42008672	322.70084422		
FES2014-O1	48.01605700	237.07245900	2.26764277	67.21390945	1.73640899	103.59443219	10.43638295	54.56971711		

Figure 5: The results of the convolutions of PREM LGFs with FES2014b ocean-tide models. This data is produced for all 3 tides and is given in terms of amplitude (mm) and phase (deg).

As Figure 5 shows, the convolution results are provided in amplitude and phase, which fully represent the surface displacements for each tidal harmonic. Once the convolutions are performed, the data is passed to a LoadDef program called env2pme.py to convert this data to PME format, which can be plotted as PMEs in the GMT software (Wessel et al., 2013).

In this study, a CM reference frame was used for analysis and calculations. The CM reference frame is a reference frame that accounts for the Earth's fluids and is in reference to Earth's center of mass (Desai & Ray, 2014). Originally, the degree-1 LLN is computed in the CE reference frame, which references the solid Earth centre of mass (Blewitt, 2003). We convert to the CM reference frame before calculating LGFs. The CM reference frame was used because the observations from the GPS orbit and clock products are retrieved in a form that best fits the CM reference frame.

How LoadDef Works for Models and Convolutions

LoadDef was published by Martens et al. in 2019. LoadDef utilizes an Earth model, such as PREM, and a tide model to model the mass loading displacements. It is utilized when computing Love numbers and Green's function and when performing convolutions. To perform the discrete convolution, LoadDef creates a template grid over Earth's surface (Martens et al., 2019). This grid is centered on the point being observed. The grid resolution is the highest near a measurement station and decreases further from stations. This is because displacement values are most susceptible to change close to stations (Martens & Simons, 2020). The grid resolution can impact the predicted OTL displacements. On the template grid used, the ocean tide heights are interpolated by way of bilinear interpolation of the input model (Martens et al., 2019). The displacement LGFs are integrated across the grid cells and multiplied by load height and density in the cell (Martens et al., 2019). There is also a land-sea mask based on ETOPO1 (Amante & Eakins, 2009) applied so that land cells do not add to the ocean load.

Observed and Predicted Ocean Tidal Loading Results

Observed ocean tidal loading

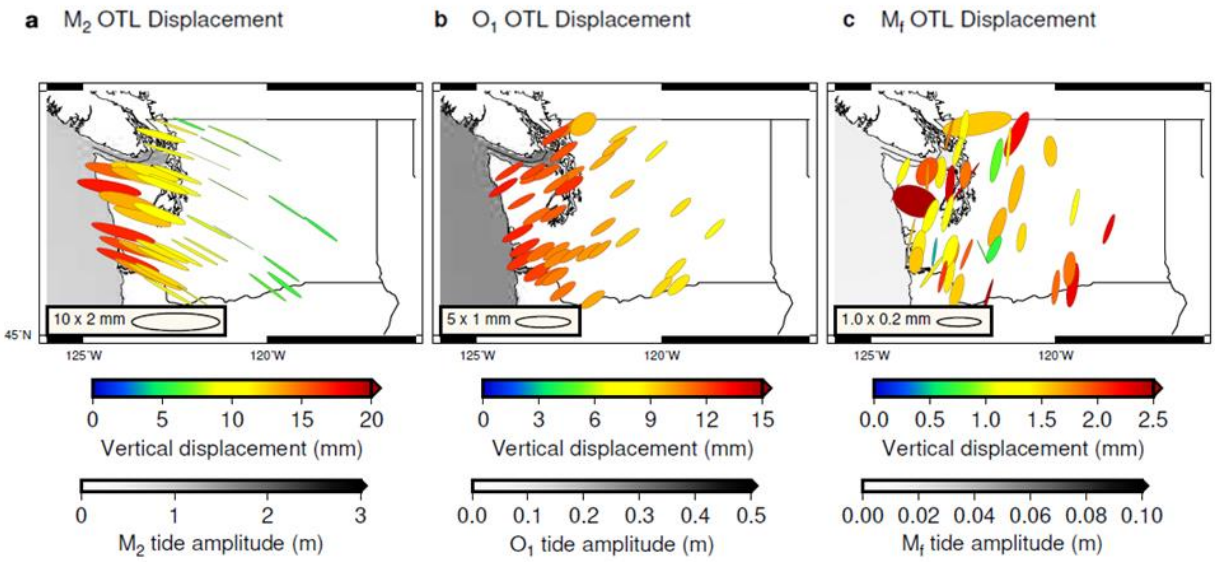

Figure 6: The observed OTL in the Puget Sound area. The plotted ellipses show the (scaled) ground track taken by the GNSS stations in response to the OTL in the area and the varying colours correspond to differing levels of vertical displacement in response to OTL. The redder an ellipse is, the more vertical displacement there is and bluer indicates less vertical displacement. The gray background shades in the ocean show the tidal amplitude. There is also a scale present, which shows what a plotted PME corresponds to in the real world, as the PMEs do not follow a path as large as the ones shown in the figure. Panel a shows the OTL due to the M_2 tide, panel b shows the OTL due to the O_1 tide, and panel c shows the OTL due to the M_f tide. This figure is produced with settings of MAD-10, WIN-14, and no sidereal filter.

The displacements of the GNSS stations are shown as particle motion ellipses (PMEs). The ellipses show the ground track of the stations, but note the scale of the ellipses, as the stations do not move hundreds of kilometres. The redder the ellipse is, the larger the vertical displacement, and a blue ellipse indicates a small vertical displacement. As shown in Figure 6, the vertical displacement is most prominent near the west coast for the M_2 and O_1 tides. There is large vertical displacement on the coast, near to the tides, and significantly less moving inland.

With the M_2 tide there are no obvious impacts that ocean tides in the Puget Sound have on the displacement of the surface due to OTL. There appears to be a continuous gradient from large displacement on the coast to less inland, with no obvious changes at the Puget Sound. The maximum vertical displacement is approximately 17 mm nearest the coast and the minimum vertical displacement is approximately 5 mm further inland. The further inland, the less impact OTL has. With the M_2 tide, the paths taken by the GPS stations, as shown by the ellipses are most broad and circular near the coast, while inland, the station moves in a more linear pattern, which is a smaller semi-minor axis. The ellipses also have a larger semi-minor axis toward the south and smaller semi-minor axis toward the north. All the ellipses are oriented in the same direction. At the coast they are nearly aligned east-west on the semi-major axis, while inland, they are getting more north facing with the semi-major axis. This direction shift occurs gradually the further inland the observations.

With the O_1 tide, the Puget Sound has an impact on vertical displacement, as there is significantly more vertical displacement at the Puget Sound and to the southeast of the Puget Sound than the surrounding areas. The displacement in the immediate area of the Puget Sound is between 11 mm and 14 mm. The scale of these ellipses is smaller, as the O_1 tide creates less vertical displacement than the M_2 tide does. Again, there is generally a pattern of less vertical

displacement inland and more displacement at the coast. The maximum vertical displacement is approximately 14 mm, and the minimum vertical displacement is approximately 6.5 mm. The ellipses are also broader here and there is no clear pattern as to the ellipse shape regarding location of the stations, as all ellipses are approximately the same shape. All the ellipses are oriented in the same direction with the semi-major axis toward the northeast.

The M_f tide's effect on vertical displacement does not appear to follow a clear pattern spatially (Figure 6). There is more displacement in the Puget Sound, but there is no clear spatial pattern for the size of ellipses or degree of displacement. The scale is significantly smaller here, as the M_f tide is very small. The maximum vertical displacement is about 2.5 mm, and the minimum vertical displacement is about 0.5 mm. The only apparent spatial pattern is that most ellipses are oriented in the same direction, with the semi-major axis aligned toward the north. However, there are outliers that do not align in the same direction, which are found close to the Puget Sound. These ellipses that are not oriented in the same direction as the others also show some of the largest vertical displacements.

Predicted OTL

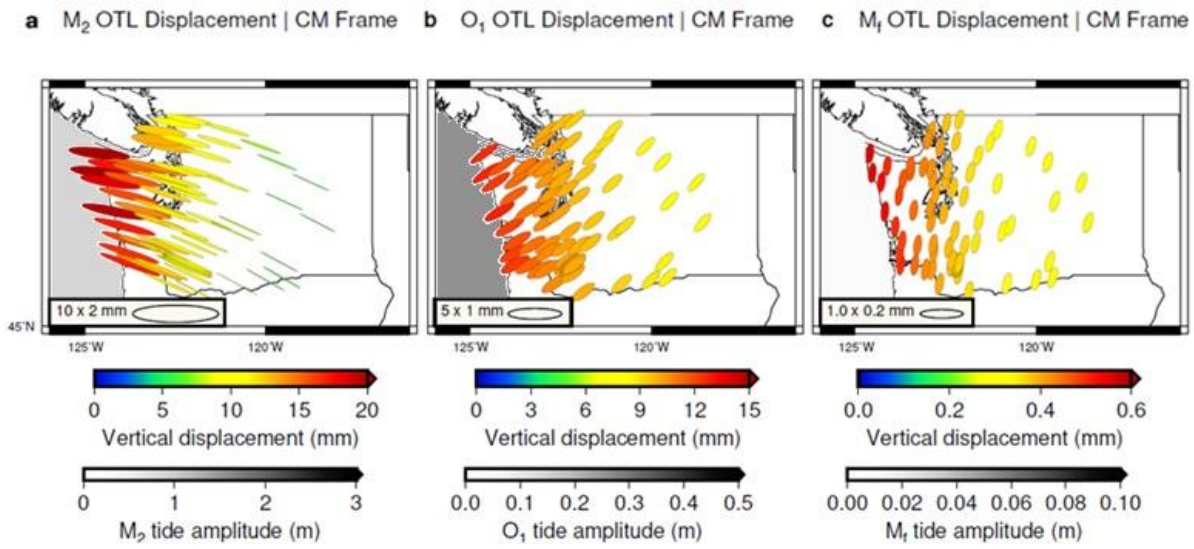

Figure 7: Model predictions of OTL in the Puget Sound area. Panel a shows the predicted OTL displacement for the M_2 tide, panel b shows predicted OTL displacement for the O_1 tide, and panel C shows predicted OTL displacement for the M_f tide. This figure assumes the FES2014b ocean-tide model and PREM structure to estimate the OTL displacements. Notably in this figure, the Puget Sound has no apparent impact on the OTL, as it shows a consistent change across the area.

The predicted OTL was done using the FES2014b model and PREM structure. These predictions are shown in Figure 7. This model utilized more stations for analysis as compared to the observations; however, only the stations used in the observations are considered for the residual's calculations (shown later).

The M_2 tide has the largest displacements, with vertical displacements between 5 and 20 mm. The largest vertical displacements are predicted along the coast and the smaller displacements

are predicted more inland. With this tide there is a clear spatial pattern with the ellipses, as the ellipses closest to the coast exhibit the largest semi-major axes, with this axis getting smaller further inland. This model predicts that the horizontal movement of the stations will be nearly linear, without a strong elliptical shape. The ellipses gradually rotate from nearly east-west alignment at the coast to approximately 45-degree rotation by the interior.

The O_1 tide is predicted to have a vertical displacement between 6 and 12 mm, with the largest displacements at the coast and getting smaller toward the interior. The movement of these stations is less than that of the M_2 tide, which makes sense as the O_1 tide is smaller. The ellipses are mostly uniform in size, regardless of location, and the majority of semi-major axes are angled in the same northeast direction.

The M_f tides are predicted to have a vertical displacement between 0.3 and 0.6 mm. This model follows the same general spatial pattern as the M_2 and O_1 tides, with the largest vertical displacements being at the coast and the smallest further inland. The ellipses are all approximately the same shape and the semi-major axes are all oriented in the same north-south direction.

Comparing Model to Observations

Figure 6 is being compared to Figure 7, which is comparing the observations to the predictions of OTL. For the M_2 tide, the ellipses in the model appear to be aligned similarly to the direction of the ellipses in the observations. They both follow the similar downward curved pattern from the coast to further inland. It also appears that the model predicts more of a vertical displacement than is observed. The coast area in the model has more vertical displacement by a few millimetres than the observations. Another obvious difference between the two is the size of

the ellipses. The ellipses in the observed data are wider on the semi-minor axis than those predicted. The ellipses near the coast are similar in size; however, further inland the observations differ more from the predictions. The ellipses are similar in central Washington, but in eastern Washington the ellipses in the model have a smaller semi-minor axis.

For the O_1 tide, the model also follows a similar spatial pattern to that seen in the observations. In both the model and the observations, the semi-major axes of the ellipses are oriented approximately east-west at the coast, but moving further inland, the semi-major axis rotates to being more northeast/southwest oriented. The vertical displacements are also very similar. The range of vertical displacements is from approximately 7.5 mm inland to 13 mm on the coast in both the model and the observations. The amount of movement of the stations are nearly the same as well, as the scale did not need to be changed for the observations or model. The biggest differences appear in the shape of the ellipses seen. The ellipses in the model are consistent in length and direction for both the semi-major and semi-minor axis, regardless of station location. They are not circular, but all the ellipses are approximately the same size and shape. The PMEs along the coast have a slightly longer semi-major axis; however, this difference is not as obvious as in the observations. In the observations it is clear that the ellipses closest to the coast have a longer semi-major axis than those seen more inland. Not all the stations follow the same ground track path for the observed data. They follow similar paths that appear the same at first; however, upon further analysis the ellipse shape varies depending on the location. This is especially evident in the most northern station, as this station follows a nearly circular path, rather than elliptical.

The M_f tide observations are very different than what the model predicts. The model predicts that the ellipses are oriented in a north-south direction and follow a clear pattern of the largest

vertical displacements at the coast and the smallest inland. In the model, the Puget Sound has no visible impact on this pattern. Also, in the model the ellipses are similar in shape to one another, regardless of location. Generally, the ellipses in the observations are oriented in the north direction predicted by the model; however, they are not all aligned in this direction. There are a few ellipses oriented in a completely different direction, but most of them are in the same general orientation. Another major discrepancy between the model and observations are the size of the ellipses. The ellipses are many different sizes in the observations, whereas in the model they are of a consistent size. Most of the ellipses in the observations are substantially larger than those of the model. Some of the ellipses have a significantly smaller semi-minor axis, but a larger semi-major axis. Another difference in this tidal frequency is the vertical displacement values. The model predicts the largest vertical displacements at the coast, while in the observations the largest vertical displacements appear random spatially. The same is true of the small vertical displacements. In the model, the smaller displacements are located further inland, while in the observations there are small displacements both close to the coast and inland. The range of vertical displacements for the model are 0.3 to 0.6 mm, while in the observations the range is from 0.75 to 2.5 mm. This is a substantial difference (factor of 2 or more), as the largest model displacements are smaller than the smallest observational vertical displacements.

Residual Displacements Between the Observed OTL and Predicted (FES2014b, PREM) OTL

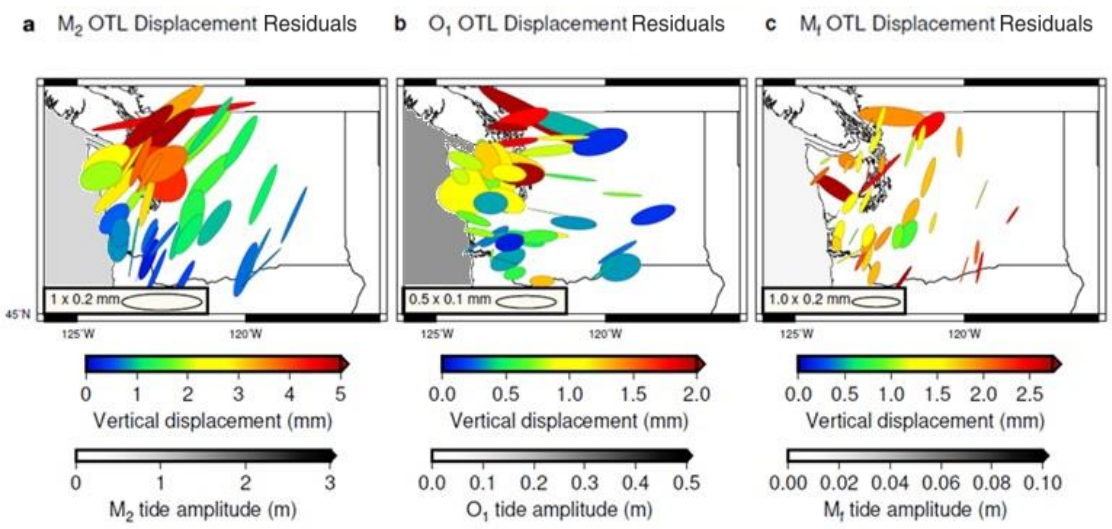

Figure 8: The residual displacements of OTL in the Puget Sound when comparing the observations to the predictions of OTL. These are the differences between the observations and the predictions of OTL. Panel a shows the residual displacements for the M_2 tide, panel b shows the residual displacements for the O_1 tide, and panel c shows the residual displacements for the M_f tide. The GPS time series used to estimate the observed OTL were filtered for outliers based on a window of 14 days and a median absolute deviation filter of 10; no sidereal filter was applied. The predictions were computed using the LoadDef software assuming PREM structure and the FES2014b ocean-tide model.

There are significant discrepancies between the observed and predicted OTL, where the predictions are based on PREM structure and the FES2014b ocean-tide model. All tides show some residuals between the predictive model and what is observed. For the M_2 and O_1 tides,

these discrepancies are largest in the Puget Sound area. For the M_f tide there does not seem to be strong spatial correlation to the Puget Sound area or the ocean. All three tides have the same period for the observations and the predictions.

For the M_2 tides the largest residuals between the model and the observations are in the immediate area of the Puget Sound. This is most likely due to deficiencies in the tide model in the Puget Sound area, which will be discussed later. The largest vertical-displacement residuals here are approximately 5mm, and the smallest are approximately 2.5 mm. These are large vertical discrepancies, compared to prior studies in other locations, which will be discussed further in the discussion. The ellipses for the M_2 tide are also large. Noting the scale change, the residual ellipses are not as large as either the predictive model or the observations; however, there are significant ground track differences. Notably, the semi-major axes of the ellipses are aligned nearly 90 degrees from the axes of the model and the observations. The ellipses are not of a consistent size in this tidal harmonic. Some of the ellipses have a long semi-major axis with a small semi-minor axis, while others have a larger semi-minor axis, and some are nearly circular. The most circular ellipses are seen in the immediate area of the Puget Sound.

The O_1 tide residuals follow a similar spatial pattern and coherency to the model and observations. The ellipses are mostly oriented with the semi-major axis in the east-west orientation. The ellipses do not vary in orientation as the model and observations do. In the northern part of Washington, the ellipses are slightly oriented to the northwest, while in the southern part of the state the are slightly oriented to the northeast. This slight change in orientation becomes less for both directions moving toward the middle of the state, and the ellipses are oriented east-west in the middle of the state. The orientation of the ellipses seem to converge in the middle of the state. The vertical displacement residuals do not follow the same

trend as the model and observations, with large displacements at the coast and smaller inland. The largest residuals in vertical displacement are seen in the northern part of the Puget Sound and the smallest residuals are seen inland and generally to the southern half of Washington. The smallest residuals are 0.1 mm, which are seen in one northern ellipse and a few ellipses in the southern half of the state. Most of the residuals in the southern portion of Washington are below 0.5 mm. The largest residuals are 2 mm, and these are seen in the immediate area of the Puget Sound. Most of the residuals in the northern part of Washington are greater than 1 mm.

The residual displacements in the M_f tide are generally oriented to the north, which is the same as the general direction of the ellipses in the observations and predictions. There are some larger ellipses that are oriented more toward the east-west direction (semi-major axis); however, these are a minority. The ellipses of the residuals are approximately the same size in the southern part of Washington and far inland. These ellipses are consistently narrower than both the observations and predictions in the eastern part of Washington. The width and length of the ellipses are mostly random in the western half of the state. In the immediate surrounding area of the Puget Sound, the residual displacement ellipses are largest. The vertical displacement residuals are seemingly random. There are small displacements immediately next to large displacement residuals. The residual vertical displacements around the Puget Sound are on the larger end of the spectrum ranging from 1.5 mm to 2.75 mm. However, these large displacement residuals are also seen inland, so there does not seem to be spatial consistency in the location of the larger or smaller vertical displacement residuals.

Observed and Predicted Ocean Tidal Loading Discussion

The observations and predictions of surface displacements induced by OTL around the Puget Sound have been derived and analyzed for the tidal harmonics M_2, O_1, and M_f. The observed OTL appears similar to the predicted OTL in all 3 tides. There is clear coherence in the M_2 and O_1 especially, as these nearly match in both figures (Figs. 6 & 7). M_f has some larger differences; however, they do not appear major when comparing the figures. The residuals between the models have been discussed above, with the largest residual vertical displacements between the observations and predictions being in the M_2 tide at 5 mm and the smallest being in the O_1 tide at 2 mm. The observed values are within 6 mm of the predicted values. When the residuals are compared to the residuals observed in similar studies, they are relatively large. In Martens & Simons (2020) looking at Alaska, the largest residuals calculated were no larger than 2 mm and in Martens et al. (2016) looking at South America the largest residuals observed were approximately 1 mm in the M_2 tide, although a harmonic common-mode component had been removed. Even the smallest residuals in this study for the O_1 tide are larger than the largest residuals in similar studies. There are several factors that could contribute to these differences, but there are likely either deficiencies in observations or in the FES2014b model. Both likely contribute, as these are large discrepancies. To determine why these residuals are as large as they are, a greater understanding is needed for both the model itself and the observations. This information would provide greater understanding into how to improve the FES2014b to fit the data more accurately. In other studies (Martens et al. 2016), it was suggested that removal of a network-coherent ‘harmonic common mode’ may be beneficial to improving interpretations of residuals. This discussion is beyond the scope of this paper; however, a likely cause of the large

residuals, at least in part, is poor modelling in the FES2014b model within the narrow and complex Puget Sound.

However, the FES2014b model likely does not account for all the errors. This model is widely regarded as a strong tide model. Other studies of OTL to refine tide models have used the FES2014b model, and in these studies the residual values between observations and predictions were smaller than in this study. This means that the model itself likely cannot explain all the variations in residual values between two studies (Martens & Simons, 2020; Martens et al., 2016), as the same model is used for both studies (albeit different geographic regions). There are other explanations for these differences. These differences could be due to geographic location. The Puget Sound has a complex coastline, tectonics, and geomorphology, as this is an active subduction zone with tectonic action. This complexity could account for some variation between this study and others. Also, as will be explained following, the tide model does not capture the entire Puget Sound, which can create large residuals. Another reasonable explanation for the differences between studies could be that in other studies the harmonic common-mode component was removed, while in this study it was not removed.

Reference-frame errors may also contribute to the discrepancies between model and observation (Fu et al., 2012; Wu et al., 2012; Desai & Ray, 2014The CM reference frame was used in the calculations of the Green's Functions as this frame works well with the data collection. The data are analyzed using the JPL orbit and clock products (final and fluidical form), which are referenced to a CM frame over long intervals. Another factor here that could contribute to the residuals is the treatment of geocenter-motion. Ocean tide models are constrained by satellite altimetry (Desai et al., 2014). For the CM frame, the sea-surface height needs to be adjusted for the variations in the geocenter due to a loading (Desai & Ray, 2014). In other studies, it was

found that if the height of the geocenter variations are accounted for on the altimetry-based sea-surface height observations, the residuals can be improved by up to 40 percent (Desai & Ray, 2014). This was found to be most prevalent in the O_1 tide. This is a degree-1 adjustment to the data, so it could influence the observed results in comparison to the model. It has been shown in Martens et al. (2016) that removing a common-mode factor can reduce the OTL-response discrepancies as a result of varying reference frames, but we do not remove a common mode here. Another error that could have occurred in the observations is with the GPS measurements themselves. GPS systems have random measurement errors, and these could influence the large residuals seen, however this factor is not analyzed in this study and should be considered and explored in future works.

The FES014b model is a finite element solution global tide model constrained by satellite altimetry (Lyard et al. 2021). This model was a significant improvement over the previous models; however, like all models, it is not perfect. For example, this model, like other global tide models, does not reach far into the Puget Sound. The model reaches into the Puget Sound somewhat; however, it does not cover the whole area. As shown in Figure 9b, the model does not consider the furthest inland part of the Puget Sound or account for the complex inland area of the Puget Sound. The model also has deficiencies along the complex coastlines of the Puget Sound. This is shown by areas of no coverage along the coast, as well as low resolution pixelation. This pixelation in Figure 9b is a result of the FES2014b model plotting on a regular grid, and the Puget Sound's coastline does not fit a regular grid. This lack of coverage and inaccuracies on the coastlines are likely sources of error. This area has the predicted OTL based on the FES2014b global tide model without full coverage of the Puget Sound. The largest residuals in all three tides are seen in the immediate Puget Sound area, and this difference could

potentially be mitigated by expanding the FES2014b model to include the Puget Sound and how the tides are moving here. Knowing how the tides within the Puget Sound are moving would likely improve the predictions of OTL around the Puget Sound and reduce the residual differences between the model and the observed data.

a)

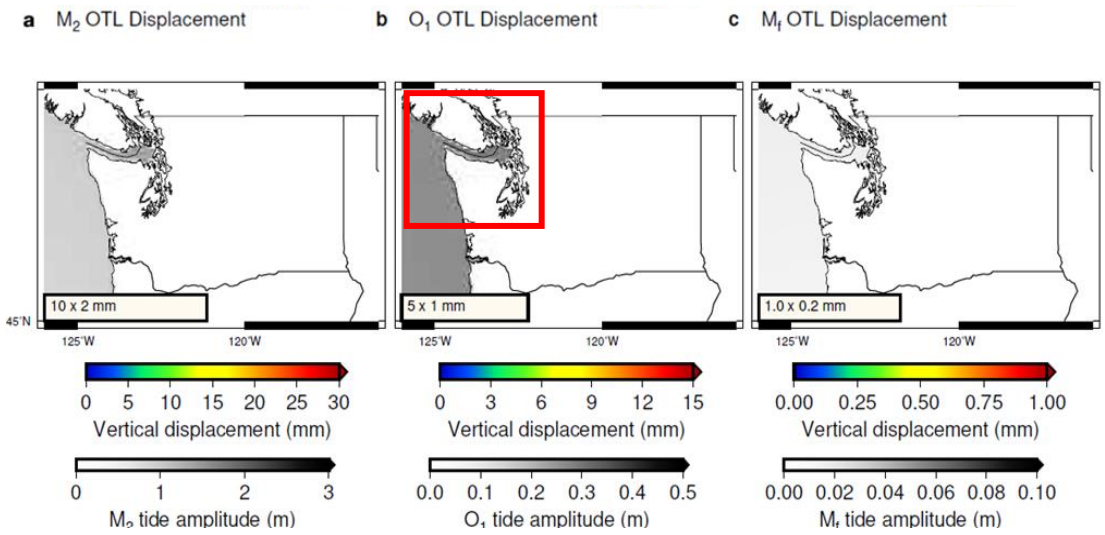

b)

Figure 9: a) Tidal model of the Pacific Ocean. The varied shades of gray show the tidal amplitude, with darker gray showing a larger amplitude. b) The tides in the Puget Sound, zoomed in on the square shown in Fig. 9a. This shows that the tidal model does not intrude far into the Puget Sound, as most of the Sound is not shaded at all. The water areas most inland

have no shading. Also of note is the pixelation near the coastlines. This shows where the model is lacking – in shallow waters and around coastlines.

Other modelling factors that could create residuals between the observations and predictions is the earth model chosen and the Earth body tide model used. I hypothesize that the choice of which SNREI earth model used would create minor changes in the model; however, it can still have an effect. It has been shown that the choice of earth model can influence changes slightly, generally around 0.1 mm (Martens et al. 2016; Martens & Simons 2020; Xu & Sun, 2003). This would have little effect on the residuals seen in this study, but it could slightly improve the comparison of the observations to the predictions. An analysis of the effects of SNREI structure on OTL residuals in the Puget Sound area is left for future work. The solid Earth body tide model was removed when going through GPS processing. However, these are long-wavelength tides, which means the residuals can have a long wavelength as well. These could contribute to the common-mode error across the network.

For the residuals of the O1 tide, it is noticeable that the PMEs follow a trend of converging at the middle of the state. The PMEs closer to the middle of the state are oriented east-west, while the PMEs at the top and bottom point toward the middle of the state and follow a trend of becoming more east-west oriented toward the center of the state, following a smooth pattern, as seen in Figure 8b. These seem to converge on the Columbia River, which flows through Washington. One reason for this could be unmodeled tides in the Columbia River. The Columbia River does have tides and these tides have been rapidly changing due to low water levels in the summer (Jay et al. 2011). The tides in this river can reach nearly half a foot at the coast, and river tides are not accounted for in the OTL analysis. These tides could be creating residuals between the

observations and the predictions in the OTL model, especially the direction the ellipses take, as they are not accounted for. There is little work done on how far the tides reach inland. This likely does not have a major impact, as there is little difference between the residuals and the observations further inland, but closer to the coast it may have a larger impact.

Sidereal Filter Impact Results

A sidereal filter was also considered in terms of its effect on the observed OTL. A sidereal filter utilizes the ground track repeat period of satellites to improve GPS signals and remove errors in high-rate GPS models, such as those from atmospheric delays, antenna effects, and most notably in this case multipath (Choi et al., 2004). When the filter is applied in the observations, in all three tides, the elliptical shape changes to being slightly narrower and smaller and there is less vertical displacement overall. This is most strongly observed in the M_f and O_1 tides, while there are less obvious differences in the M_2 tide. This is of interest because the M_2 tide is the largest of the tides, but the sidereal filter has a relatively small impact on the M_2 tide.

a)

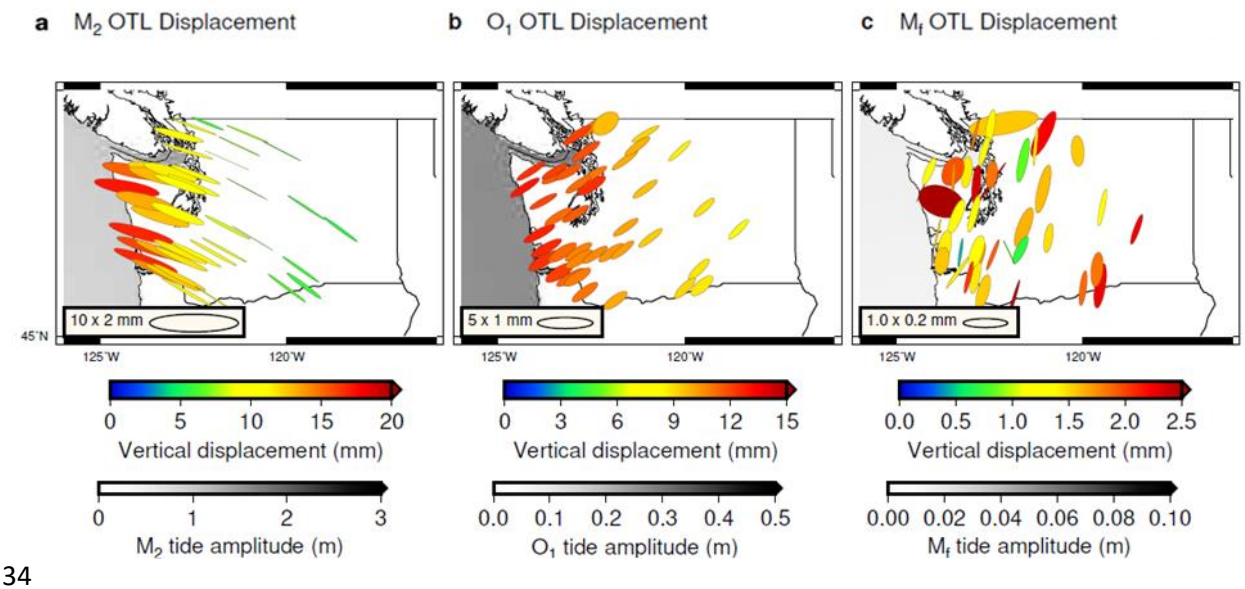

b)

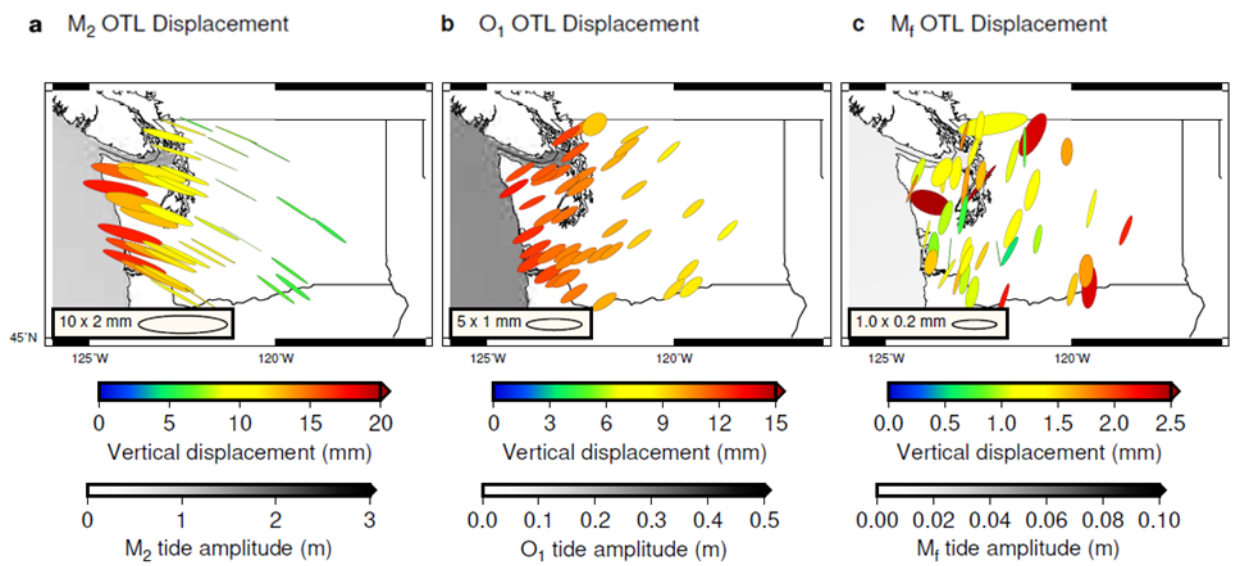

c)

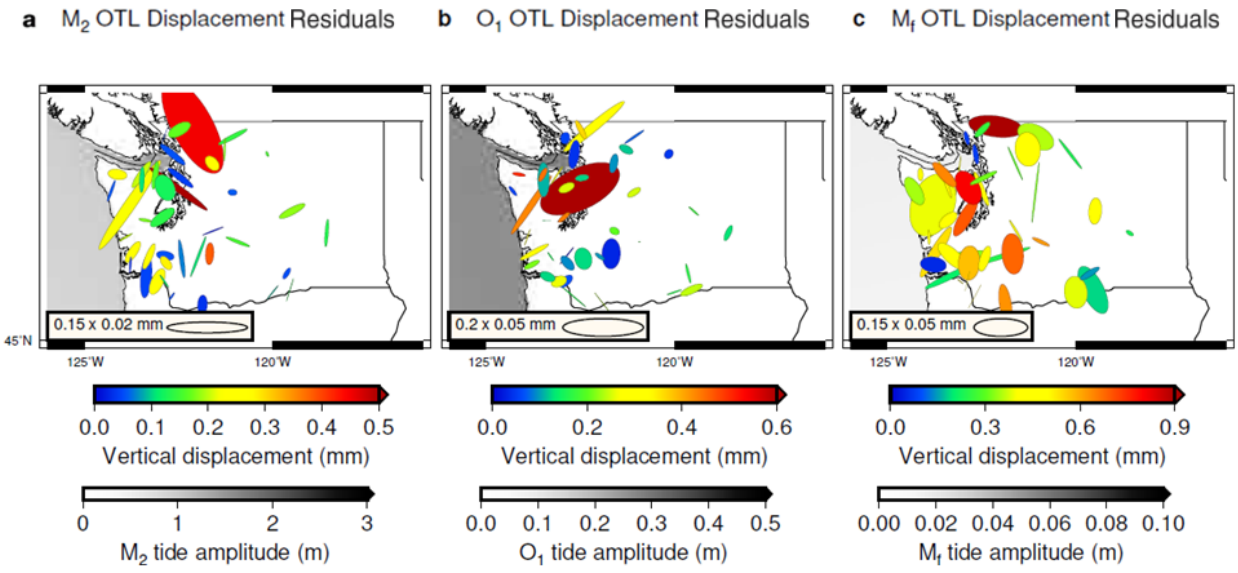

Figure 10: a) Observed surface displacements with settings of MAD-10, WIN-14, and no sidereal filter. b) Observed surface displacements with settings of MAD-10, WIN-14, and a sidereal filter applied. c) The residual difference between a lack of sidereal filter and a sidereal filter applied.

Sidereal Filter vs No Filter

The observed OTL estimated from time series without application of a sidereal filter (Figure 10a above) replicates the results shown in Figure 6. This figure was described in the 'Observed ocean tidal loading' section of this paper. Figure 10b shows the results when a sidereal filter is applied to the data. In the M_2 tide, this figure shows a spatial coherence in the direction of the ellipses, consistent with the results for no applied filter. The figure is nearly identical to the non-sidereal filter data.

The O_1 tide in the sidereal filtered data (Fig. 10b, center) is also largely consistent with the results when no filter has been applied. The data is nearly identical to the non-sidereal filter data. The biggest difference is that, when there is no filter applied there is more vertical displacement in the immediate Puget Sound area. This difference is approximately 2 mm.

The most obvious differences between the sidereal filtered data and the data not subject to a sidereal filter is in the M_f tide. Some ellipses are oriented slightly differently when the filter is applied; however, these are small changes that are difficult to detect. The differences come when analyzing the size of the ellipses and the amount of vertical displacement recorded. The ellipses are smaller when the sidereal filter is applied (network average reduction of about 0.05 - 0.1 mm narrower in filtered data). The larger PMEs are where this change is obvious, as the semi-major and semi-minor axes become visibly smaller when the filter is applied. This is most visible with the ellipses that immediately surround the Puget Sound. The sidereal filter also changes the vertical displacement values of the data. With the filter applied, the maximum vertical displacement is 2.2 mm, and the minimum is 0.5 mm. These values are similar to the maximum and minimum when there is not a sidereal filter applied (maximum vertical

displacement of 2.5 mm and a minimum of 0.7 mm); however, the average value of vertical displacement without the filter is 1.7 mm, while with the filter it is lower at 1.2 mm. This is evidence that the application of a sidereal filter can make a difference in the OTL data that is observed.

Sidereal Filter vs No Filter Residual Results

Next, we consider residuals between a sidereal filter and lack thereof. For all three harmonics, there does not seem to be spatial coherency with the residuals. They residual PMEs appear to be oriented randomly. The vertical-displacement residuals also seem to be largely random. There are some stations that have high values of vertical-displacement residual immediately next to stations that have low values of vertical-displacement residual. It is important to note the scales in the residual panels (Fig.10c), as they are significantly smaller than the scales used to plot the observed displacement (Figs. 10a, b). The largest residuals between a sidereal filter and not occur with the M_f tide at 0.9 mm. This is interesting, as this is the smallest of the tides, but the large residuals suggest a sensitivity to the sidereal filter. The largest differences tend to occur near the Puget Sound. The maximum vertical-displacement residual in the M_2 tide is 0.5 mm and the minimum is 0.01 mm. The maximum of the vertical-displacement residual for the O_1 tide is 0.6 mm and the minimum is 0.01 mm. The maximum vertical-displacement residual for the M_f tide is 0.9 mm and the smallest is 0.05 mm.

Sidereal Filter Discussion

The impacts of applying a sidereal filter to observations of OTL was analyzed. This was compared to the same observations without a sidereal filter applied. The largest maximum residuals were seen in the M_f tide at 0.9 mm and the smallest maximum residuals were in the M_2 tide at 0.5 mm. These are not insignificant values, but they are small relative to the residuals between predicted and observed OTL (Fig. 8). In the studies performed by Martens et al. (2016) and Martens & Simons (2020), the residuals of the observations compared to the models were sub-millimeter, which is on par with the residuals found here between observations of OTL derived with and without a sidereal filter.

Multipath errors alter the data produced in a GPS experiment, as was performed here. In experiments testing the effectiveness of a sidereal filter it was found that sidereal filters reduce the amount of noise seen in GPS data (Itoh & Aoki, 2022). Recent studies have shown that sidereal filters can have data fluctuations less than 6 mm in standard deviation, which means there is less noise and cleaner data for GPS positions (Itoh & Aoki, 2022). However, caution must be exercised when applying a sidereal filter, depending on the application. In the case of tides, the filter overlaps in frequency space with the tidal harmonics and can therefore manipulate the OTL results. If a sidereal filter is applied, the amplitude and phase of the tidal signals are affected.

If a sidereal filter is applied, it does clean up the multipath errors and tighten the data, but it may be inadvertently manipulating the tidal amplitudes and phases. The use of the filter should be carefully considered and explored further to quantify and assess the impacts on tidal estimates.

Conclusion

In this study, the forward-modelled predictions of OTL are compared to observations of OTL produced by GNSS data in the Puget Sound area. This was done to explore Earth's elastic deformation response to OTL. Data was collected from GNSS stations in Washington and was processed to give position estimates of the GNSS stations at intervals of 5 minutes for a year. This was done for the tidal frequency bands M_2, O_1, and M_f. The maximum residuals determined for the M_2 tide were 5 mm, the O_1 2 mm, and the M_f 2.75 mm. These are relatively large values compared to the values seen in similar studies, albeit a harmonic common mode has not been removed here. Spatial coherency in the residuals, and relatively large residuals around the Puget Sound, suggest that there may be local-scale room for improvement in the FES2014b tide model that was used in the analysis (particularly the model representation of tides in the Puget Sound), the PREM model for Earth structure, the observations of OTL, or all three. We hypothesize that limitations in coverage in the FES2014b tide model within the Puget Sound contribute significantly to the residuals in that area. This is thought because the largest residuals are seen in the immediate area of the Puget Sound. The FES2014b model does not extend far into the Puget Sound, so the tides here are not considered in the predicted OTL displacements. The model likely needs to be expanded to include the Puget Sound to have less residual displacement between the predictive model and the observations.

Also considered in this study was the use of a sidereal filter and quantifying the difference between the data produced when a sidereal filter is used versus when it is not. It was determined that the largest residual between the use of a sidereal filter and not in the M_2 tide was 0.5 mm, the O_1 tide was 0.6 mm, and the M_f tide was 0.9 mm. These values are smaller than the residuals

between observed and predicted OTL but not insignificant, suggesting that OTL observations are sensitive to the application of a sidereal filter. The application of a sidereal filter should be further explored to precisely determine the impacts on OTL observations and the advantages and disadvantages of applying the filter.

Future Works

The first avenue that should be explored in a future work is the impact that common-mode errors, as well as a network-coherent harmonic common mode, have on the observations of data. Quantifying the effect that this has on the results would likely reduce the residuals between the FES2014b model and the observations. Once the residuals are computed, this data can be used to refine the FES2014b model for better predictions of OTL around the Puget Sound.

Another way that this work could be continued is to perform the comparisons of predictive models with observed data but using a different tidal model. There are several tidal models available, including FES2012, TPXO9-Atlas, EOT11A, and GOT4.10c. This research could be continued by comparing these tidal models in the same way that FES2014b was compared with in this study. The FES2014b model could be also used again but using a CF or CE frame instead of a CM frame. This would change the reference frame used in the predicted models, which would affect the results of the observations compared to the predictions. Other models of Earth structure could also be explored.

Another way this project could be continued is to explore a sidereal filter further. This could be the same methodology applied in another location to see if the results are similar. The analysis

of how much overlap there is in the frequency of multipath errors and tidal frequencies should also be studied before a sidereal filter is used as common practice in OTL analysis.

Works Cited

Agnew, D.C., 2015, Earth tides, in Treatise on Geophysics: Schubert G., Elsevier B.V., p. 151-178.

Amante, C., and Eakins, B.W., 2009, ETOPO1 1 arc-minute global relief model.

Atkins, C., and Ziebart, M., 2015, Effectiveness of observation-domain sidereal filtering for GPS precise point positioning: GPS Solutions, v. 20, p. 111-122, doi: 10.1007/s10291-015-0473-1.

Bertiger, W., Bar-Sever, Y., Dorsey, A., Haines, B., Harvey, N., Hemberger, D., Heflin, M., Lu, W., Miller, M., Moore, A.W., Murphy, D., Ries, P., Romans, L., Sibois, A., Sibthorpe, A., Szilagyi, B., Vallisneri, M., and Willis, P., 2020, GipsyX/RTGx, a new tool set for space geodetic operations and research: Advances in Space Research, v. 66, p. 469-489, doi: 10.1016/j.asr.2020.04.015.

Blewitt, G., 2003, Self-consistency in reference frames, geocenter definition, and surface loading of the solid Earth: Journal of Geophysical Research: Solid Earth, v. 108, p. 2103-n/a, doi: 10.1029/2002JB002082.

Bos, M.S., Penna, N.T., Baker, T.F., and Clarke, P.J., 2015, Ocean tide loading displacements in western Europe: 2. GPS-observed anelastic dispersion in the asthenosphere: Journal of Geophysical Research. Solid Earth, v. 120, p. 6540-6557, doi: 10.1002/2015JB011884.

Brosche, P., Sündermann, J., Bonatz, M., Calame, O., Enslin, H., Lambeck, R., Morrison, L.V., Mulholland, J.D., and Piper, J.D., 1978, Tidal Friction and the Earth's Rotation: Berlin, Heidelberg, Springer Berlin / Heidelberg.

Brown, R.D., and Hutchinson, M.K., Ocean Tide Determination from Satellite Altimetry, in Oceanography from Space: Boston, MA, Springer US, p. 897-906.

Carrère L., Lyard F., Cancet M., Guillot A., Roblou L., 2012. FES2012: a new global tidal model taking advantage of nearly 20 years of altimetry, in Proceedings of meeting “20 Years of Altimetry”, Venice.

Choi, K., Bilich, A., Larson, K.M., and Axelrad, P., 2004a, Modified sidereal filtering: Implications for high-rate GPS positioning: Geophysical Research Letters, v. 31, p. L22608-n/a, doi: 10.1029/2004GL021621.

Choi, K., Bilich, A., Larson, K.M., and Axelrad, P., 2004b, Modified sidereal filtering: Implications for high-rate GPS positioning: Geophysical Research Letters, v. 31, p. L22608-n/a, doi: 10.1029/2004GL021621.

Desai, S.D., and Ray, R.D., 2014a, Consideration of tidal variations in the geocenter on satellite altimeter observations of ocean tides: Geophysical Research Letters, v. 41, p. 2454-2459, doi: 10.1002/2014GL059614.

Desai, S.D., and Ray, R.D., 2014b, Consideration of tidal variations in the geocenter on satellite altimeter observations of ocean tides: Geophysical Research Letters, v. 41, p. 2454-2459, doi: 10.1002/2014GL059614.

Dong, D., Wang, M., Chen, W., Zeng, Z., Song, L., Zhang, Q., Cai, M., Cheng, Y., and Lv, J., 2015, Mitigation of multipath effect in GNSS short baseline positioning by the multipath hemispherical map: Journal of Geodesy, v. 90, p. 255-262, doi: 10.1007/s00190-015-0870-9.

Dziewonski, A.M., and Anderson, D.L., 1981, Preliminary reference Earth model: Physics of the Earth and Planetary Interiors, v. 25, p. 297-356, doi: 10.1016/0031-9201(81)90046-7.

Foreman, M.G.G., Crawford, W.R., Cherniawsky, J.Y., Henry, R.F., and Tarbotton, M.R., 2000, A high-resolution assimilating tidal model for the northeast Pacific Ocean: Journal of Geophysical Research: Oceans, v. 105, p. 28629-28651, doi: 10.1029/1999JC000122.

Fu, Y., Freymueller, J.T., and van Dam, T., 2011, The effect of using inconsistent ocean tidal loading models on GPS coordinate solutions: Journal of Geodesy, v. 86, p. 409-421, doi: 10.1007/s00190-011-0528-1.

Hannah, B.M., 2001, Modelling and Simulation of GPS Multipath Propagation [Ph.D. thesis]: Queensland University of Technology.

Herring, T.A., Melbourne, T.I., Murray, M.H., Floyd, M.A., Szeliga, W.M., King, R.W., Phillips, D.A., Puskas, C.M., Santillan, M., and Wang, L., 2016, Plate Boundary Observatory and related networks: GPS data analysis methods and geodetic products: Reviews of Geophysics (1985), v. 54, p. 759-808, doi: 10.1002/2016RG000529.

Ito, T., and Simons, M., 2011, Probing Asthenospheric Density, Temperature, and Elastic Moduli Below the Western United States: Science (American Association for the Advancement of Science), v. 332, p. 947-951, doi: 10.1126/science.1202584.

Itoh, Y., and Aoki, Y., 2022, On the performance of position-domain sidereal filter for 30-s kinematic GPS to mitigate multipath errors: Earth, Planets, and Space, v. 74, p. 1-20, doi: 10.1186/s40623-022-01584-8.

Jay, D.A., Leffler, K., and Degens, S., 2011, Long-Term Evolution of Columbia River Tides: Journal of Waterway, Port, Coastal, and Ocean Engineering, v. 137, p. 182-191, doi: 10.1061/(ASCE)WW.1943-5460.0000082.

Jentzsch, G., 2005, Earth tides and ocean tidal loading, in Tidal Phenomena: Berlin, Heidelberg, Springer Berlin Heidelberg, p. 145-171.

Lawler, G.F., and Limic, V., 2010, Random Walk: A Modern Introduction: Cambridge, Cambridge University Press.

Lichtenegger, H., Wasle, E., and Hofmann-Wellenhof, B., GNSS Global Navigation Satellite Systems: GPS, GLONASS, Galileo, and more: Vienna, Springer Vienna.

Lyard, F.H., Allain, D.J., Cancet, M., Carrère, L., and Picot, N., 2021, FES2014 global ocean tide atlas: design and performance: Ocean Science, v. 17, p. 615-649, doi: 10.5194/os-17-615-2021.

Martens, H.R., and Simons, M., 2020, A comparison of predicted and observed ocean tidal loading in Alaska: Geophysical Journal International, v. 223, p. 454-470, doi: 10.1093/gji/ggaa323.

Martens, H.R., Rivera, L., and Simons, M., 2019, LoadDef: A Python-Based Toolkit to Model Elastic Deformation Caused by Surface Mass Loading on Spherically Symmetric Bodies: Earth and Space Science (Hoboken, N.J.), v. 6, p. 311-323, doi: 10.1029/2018EA000462.

Martens, H.R., Rivera, L., Simons, M., and Ito, T., 2016, The sensitivity of surface mass loading displacement response to perturbations in the elastic structure of the crust and mantle: Journal of Geophysical Research. Solid Earth, v. 121, p. 3911-3938, doi: 10.1002/2015JB012456.

Martens, H.R., Simons, M., Owen, S., and Rivera, L., 2016, Observations of ocean tidal load response in South America from subdaily GPS positions.

Mohamed, A.S., Doma, M.I., and Rabah, M.M., Study the Effect of Surrounding Surface Material Types on the Multipath of GPS Signal and Its Impact on the Accuracy of Positioning Determination: American Journal of Geographic Information System, v. 2019, p. 199.

Ozawa, I., 1957, Study on Elastic Strain of the Ground in Earth Tides: Bulletins - Disaster Prevention Research Institute, Kyoto University, v. 15, p. 1-36.

Pain, C.C., Piggott, M.D., Goddard, A.J.H., Fang, F., Gorman, G.J., Marshall, D.P., Eaton, M.D., Power, P.W., and de Oliveira, C.R.E., 2005, Three-dimensional unstructured mesh ocean modelling: Ocean Modelling (Oxford), v. 10, p. 5-33, doi: 10.1016/j.ocemod.2004.07.005.

Polagye, B., and Thomson, J., 2013, Tidal energy resource characterization: methodology and field study in Admiralty Inlet, Puget Sound, WA (USA): Proceedings of the Institution of Mechanical Engineers. Part A, Journal of Power and Energy, v. 227, p. 352-367, doi: 10.1177/0957650912470081.

Pugh, D., and Woodworth, P., 2014, Sea-Level Science: Cambridge University Press.

Wahr, J.M., 1981, Body tides on an elliptical, rotating, elastic and oceanless earth: Geophysical Journal International, v. 64, p. 677-703, doi: 10.1111/j.1365-246X.1981.tb02690.x.

Wessel, P., Smith, W.H.F., Scharroo, R., Luis, J., and Wobbe, F., 2013, Generic Mapping Tools: Improved Version Released: Eos (Washington, D.C.), v. 94, p. 409-410.

Wu, X., Ray, J., and van Dam, T., 2012, Geocenter motion and its geodetic and geophysical implications: Journal of Geodynamics, v. 58, p. 44-61, doi: 10.1016/j.jog.2012.01.007.

Xu, J., and Sun, H., 2003, Deformation Response of a Snrei Earth to Surface Loads and Tidal Forces: Chinese Journal of Geophysics, v. 46, p. 465-477, doi: 10.1002/cjg2.3364.

Zhdanov, A., Zhodzishsky, M., Veitsel, V., and Ashjaee, J., 2002, Evolution of Multipath Error Reduction with Signal Processing: GPS Solutions, v. 5, p. 19-28, doi: 10.1007/PL00012896.

Zschau, J., 1978, Tidal Friction in the Solid Earth: Loading Tides Versus Body Tides, in Tidal Friction and the Earth's Rotation: Berlin, Heidelberg, Springer Berlin Heidelberg, p. 62-94.

Appendix 1

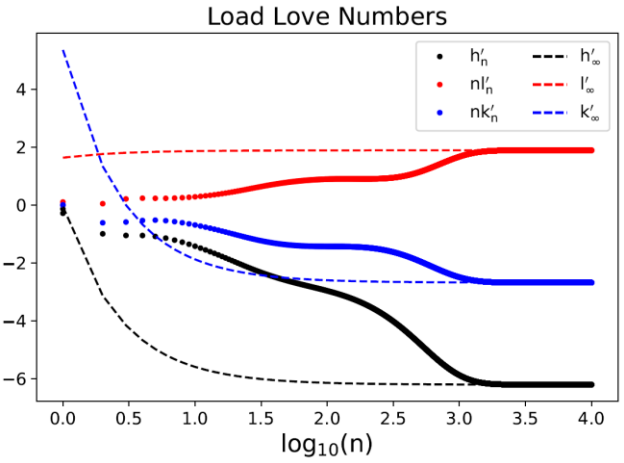

Figure 10: Graphical depiction of the LLNs used in computing predictions of OTL. The LLNs are based on PREM structure. LLNs are used to characterize the rigidity of the planet and how easily it changes shape due to tidal loading. They are used in the production of Green's Functions.

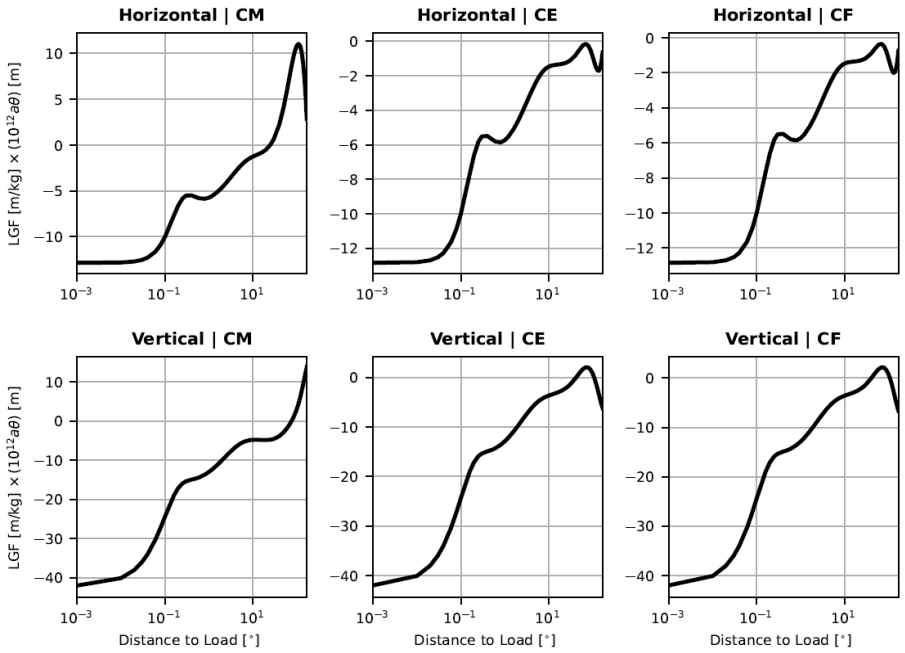

Figure 11: Graphical depiction of the LGFs used in computing predictions of OTL. This computation was done for the vertical and horizontal displacement. The LGFs are based on PREM structure.